

Cellulose-Based Flexible Organic Light-Emitting Diodes with Enhanced Stability and External Quantum Efficiency

Qinghong Zheng,^{# a, b, c} Huixin Li,^a Yiling Zheng,^a Yanan Li,^a Xi Liu,^a Shuangxi Nie,^b Xinhua Ouyang,^{* a} Lihui Chen^a and Yonghao Ni^{a, d}

^a College of Materials Engineering, Fujian Agriculture and Forestry University, Fuzhou 350002, People's Republic of China.

^b Guangxi Key Laboratory of Clean Pulp & Papermaking and Pollution Control, School of Light Industry and Food Engineering, Guangxi University, Nanning 530004, People's Republic of China.

^c National Forestry & Grassland Administration Key Laboratory for Plant Fiber Functional Materials, Fuzhou 350002, People's Republic of China.

^d Department of Chemical Engineering, University of New Brunswick, Fredericton, New Brunswick, Canada E3B 5A3.

* E-mail address: ouyangxh@fafu.edu.cn

E-mail address: fafuzqh@163.com.

1. The Fabrication process of RCF

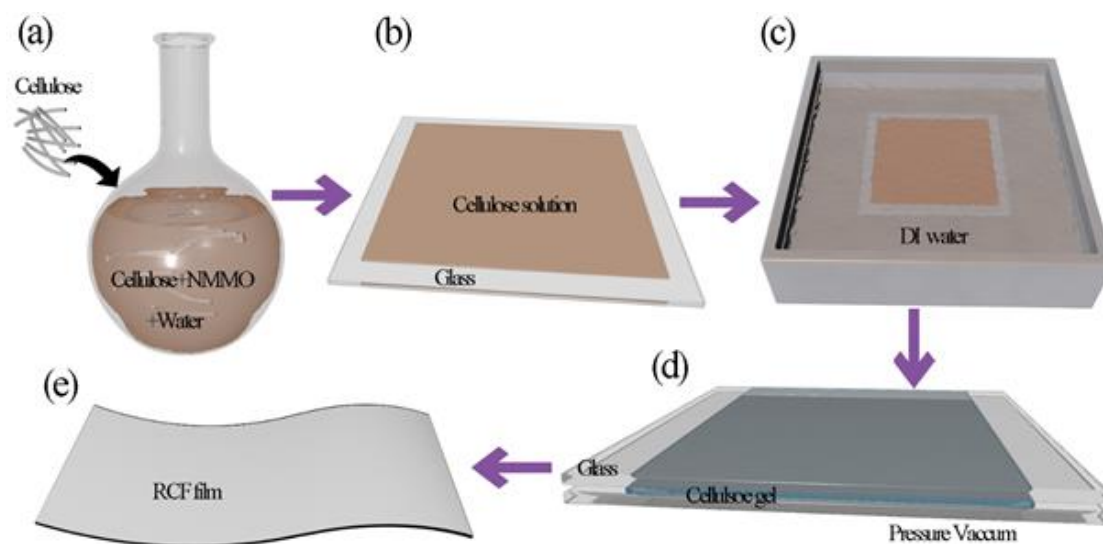


Figure S1. The detailed preparation process of regenerated cellulose film. (a) Cellulose dissolving. (b) Coating of cellulose solution. (c) Removing the NMMO solvent. (d) Drying of cellulose film. (e) The prepared regenerated cellulose film.

Figure S1 shows the detailed preparation process of the regenerated cellulose film. Firstly, *N*-methylmorpholine-*N*-oxide (NMMO) powder, a small amount of antioxidant propyl gallate (PG) and deionized (DI) water were added into a round bottom flask, and stirred with a magnetic rotor at a temperature of 110 °C. After about 10 minutes, NMMO was completely dissolved. Next, the cellulose powder was added to the NMMO solvent, and stirring continued for 4 hours at a temperature of 110 °C to obtain a uniform and stable cellulose-NMMO solution, as shown in figure S1(a). The cellulose-NMMO solution was coated on a clean glass plate with a coater to form a cellulose-NMMO gel film, as shown in figure S1(b). And then, the cellulose gel film and the glass plate are put into DI water to remove the NMMO solvent to obtain a pure cellulose gel film, as shown in figure S1(c). The cellulose gel film was sandwiched between two glass plates and placed in a vacuum drying oven at 40°C for 12 hours at a constant temperature to obtain finally a dry and transparent regenerated cellulose film (RCF), as shown in figure S1(d)-(e).

2. The preparation of PH1000/RCF composite electrode

In order to prepare high conductivity anode, the PEDOT:PSS PH1000 (PH1000) solution was pretreated with ethylene glycol (EG) of different volume ratios and spin-coated on the cellulose film by a homogenizer to form a PH1000/RCF composite film, which was annealed at different temperatures. The relationship between sheet resistance, light transmittance and volume ratios of EG are shown in figure S2 (a). With the increase of EG volume ratios, the sheet resistance of PH1000 first decreases and then increases, with a minimum value at 6%. However, the transmittance of PH1000 remains relatively stable with the increase of EG volume ratios. Figure S2(b) shows the relationship between the sheet resistance and annealing temperature of the 1-layer PH1000 electrode. When annealed at 130 °C, the PH1000 film exhibits a lowest sheet resistance. In summary, when the volume ratio of EG is 6% and the annealing temperature is 130 °C, the PH1000/RCF composite electrode has the best photoelectric performance.

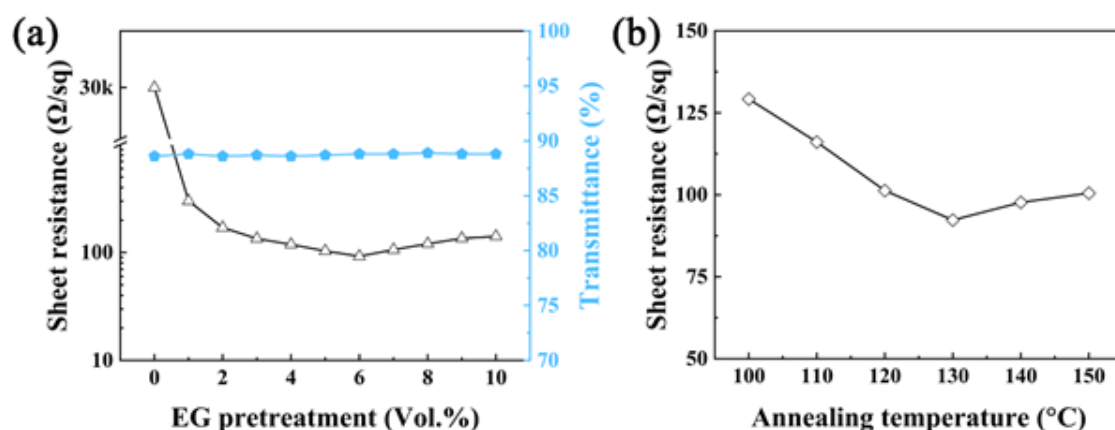
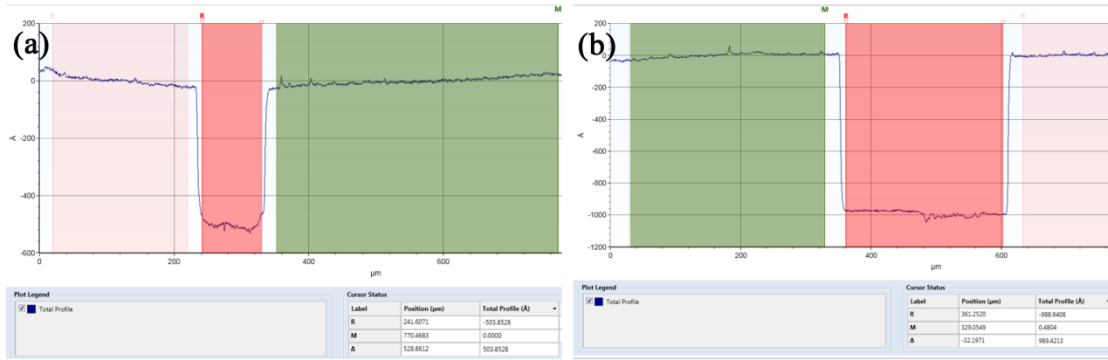


Figure S2. (a) The relation diagram between sheet resistance, light transmittance (1-layer PH1000) and pretreatment with different volumes of ethylene glycol. (b) The relation diagram of sheet resistance (1-layer PH1000) and different annealing temperature.

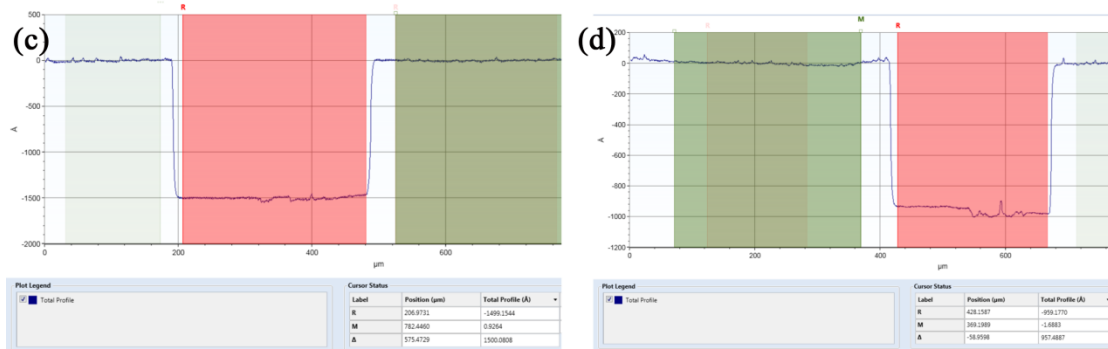
3. Thickness measurement of each layer of the device

The thickness of each layer of the device was characterized by a probe-type surface profiler (Dektak XT, Bruker Analytical Instruments). The relevant data is shown in the figure below. As shown in figure S3, the thickness of 1-layer, 2-layer and 3-layer PH1000 electrodes, and indium tin oxide (ITO) electrode are 50.4, 98.9, 150.0 and 95.7 nm, respectively. And as shown in figure S4, the thickness of Al4083, Alq3, NPB and Al are 50.3, 41.6, 39.1 and 101.5 nm, respectively.



1-layer PH1000

2-layer PH1000



3-layer PH1000

ITO

Figure S3. The screenshot of measuring the thickness of each layer (a) 1-layer PH1000, (b) 2-layer PH1000, (c) 3-layer PH1000, and (d) ITO.

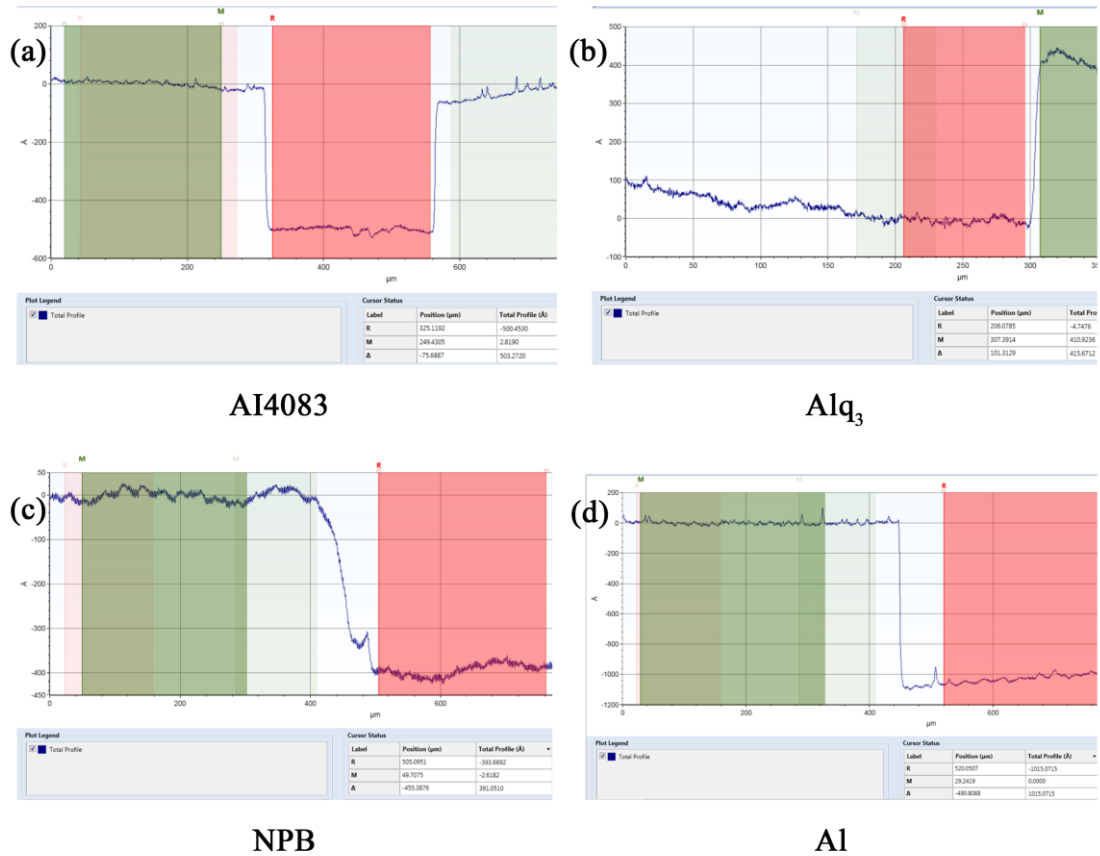


Figure S4. The screenshot of measuring the thickness of each layer (a)AI4083, (b)Alq₃, (c) NPB, and (d) Al.

4. The adhesion strength of ITO and PH1000 to the RGC substrate measured using the standard Pull-off method

The adhesion strength of ITO and PH1000 to the RGC substrate was measured using the standard Pull-off method, to evaluate the compactness between the transparent conductive electrodes and the RCF substrate. The schematic drawing and real-time graph of the measurements are shown in figure S5 (a) and (b). Briefly, first, the RGC and coating sides of the sample were bound to the ends of two metal rods with double-sided tape (3M™ VHB). Then, a gradually increasing tensile force is applied to the other end of the two rods using a tensile testing machine (KJ-1065, Kejian Tech Co., Ltd.). The adhesion strength is defined as the adhesion force per unit area corresponding to the moment of breakage at the bond.

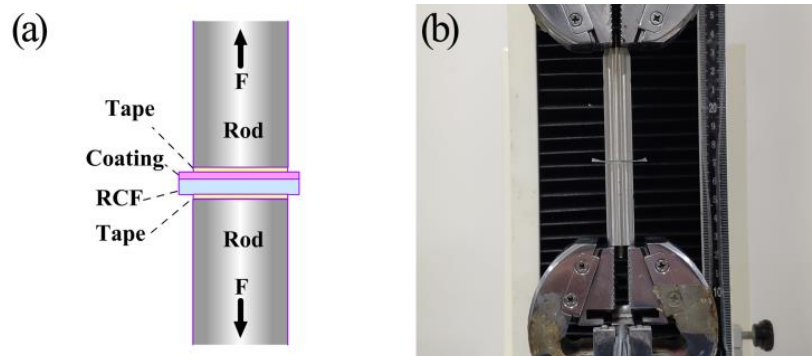


Figure S5 (a) Schematic diagram and (b) real-time graph of the pull-off test.

5. Bending test with various radiuses.

No cracks were observed in the as-deposited ITO film on RCF substrate, as shown in figure S6 (a). The microscopic photographs of the ITO/RCF films after 100 bends with bending radii of 10 mm, 6 mm and 4 mm are shown in (b), (c) and (d), respectively. It can be seen that cracks can already be observed even at relatively large bending radii (10 mm). As the bending radius decreases, the density of cracks increases and the crack width becomes larger. The cracks are ascribed to the inherent brittleness of ITO film, and are responsible for the drastic decrease in the conductivity of the ITO/RCF electrode. In contrast, such cracks were not observed in the PH1000/RCF samples after bending under the same conditions, as shown in figure S7.

It is worth noting that if ITO/RCF is simply fixed with a bending radius of 6 mm without being repeatedly bent, ITO does not show significant cracks.

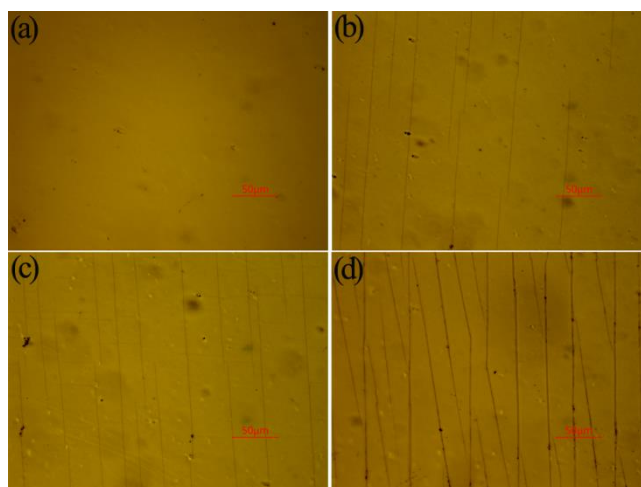


Figure S6. Microscope photos of the surfaces of ITO/RCF films bended for 100 cycles. Without bending (a), and with bending radius of (b) 10 mm, (c) 6 mm and (d) 4 mm.

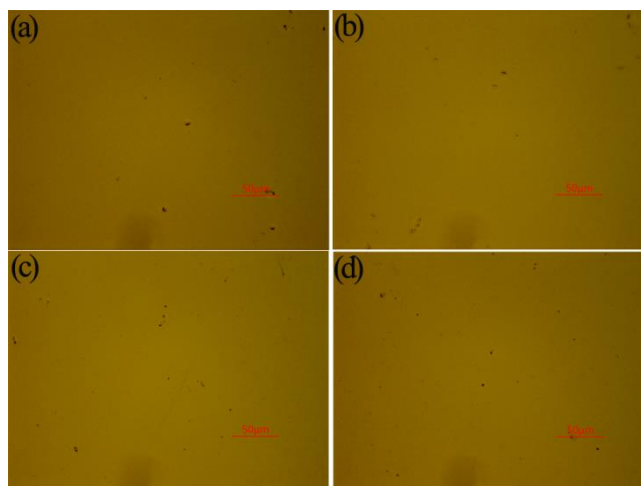


Figure S7. Microscope photos of the surfaces of PH1000/RCF films bended for 100 cycles. Without bending (a), and with bending radius of (b) 10 mm, (c) 6 mm and (d) 4 mm.

6. The J-V-L curves for PH1000-OLED and ITO-OLED devices from 6 batches.

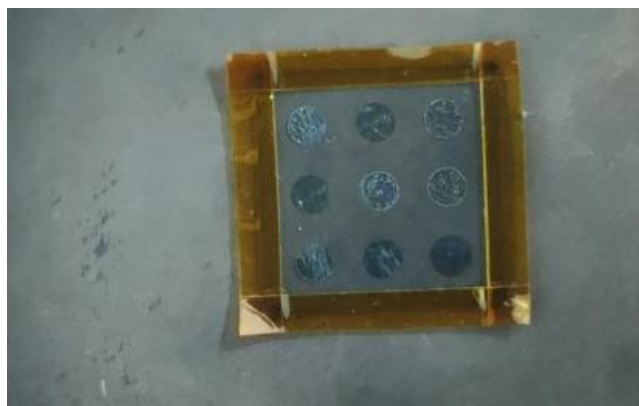


Figure S8. Digital photo of 9 devices prepared on a substrate.

The substrates used are $2.5 \times 2.5 \text{ cm}^2$, and nine devices can be prepared on each substrate, as shown in figure S8. Six batches of samples were prepared under optimal conditions to test the repeatability of fabrication of OLED based on cellulose substrate. For comparison, the three samples are taken from the center, edge and corner of each batch. The J-V-L curves for these PH1000-OLED and ITO-OLED devices are shown in figure S9 and figure S10.

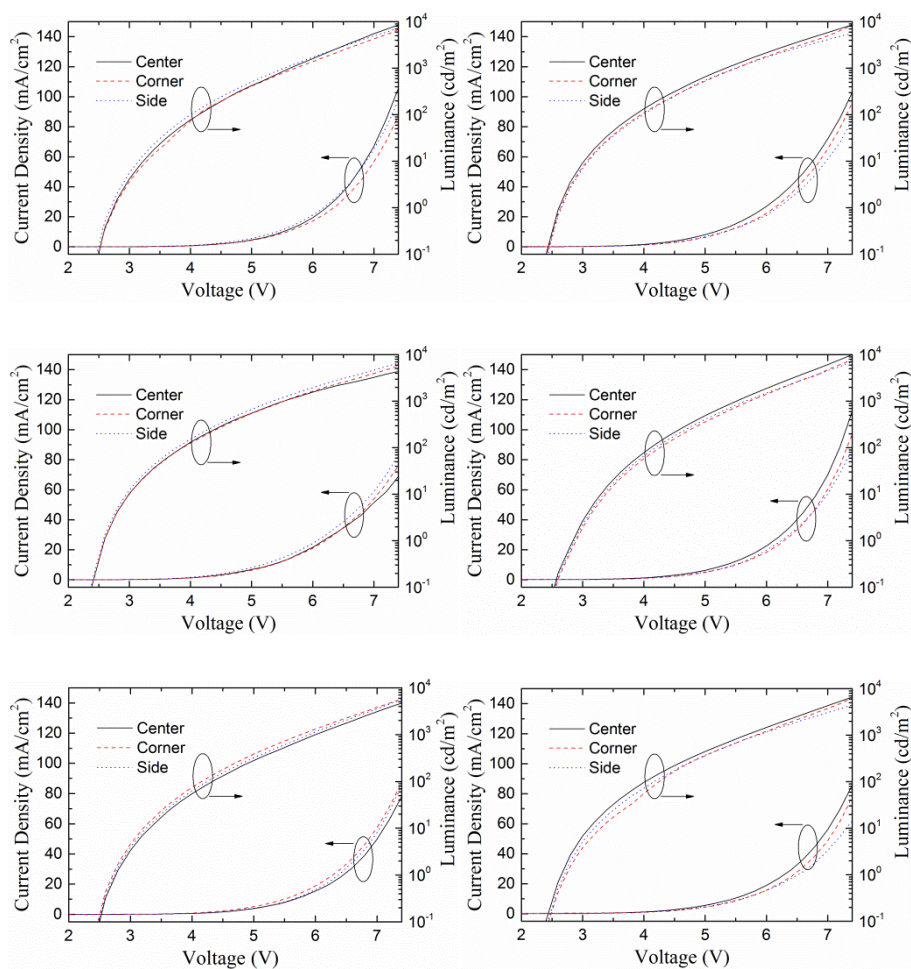


Figure S9 J-V-L curve of 18 ITO-OLED from 6 batches.

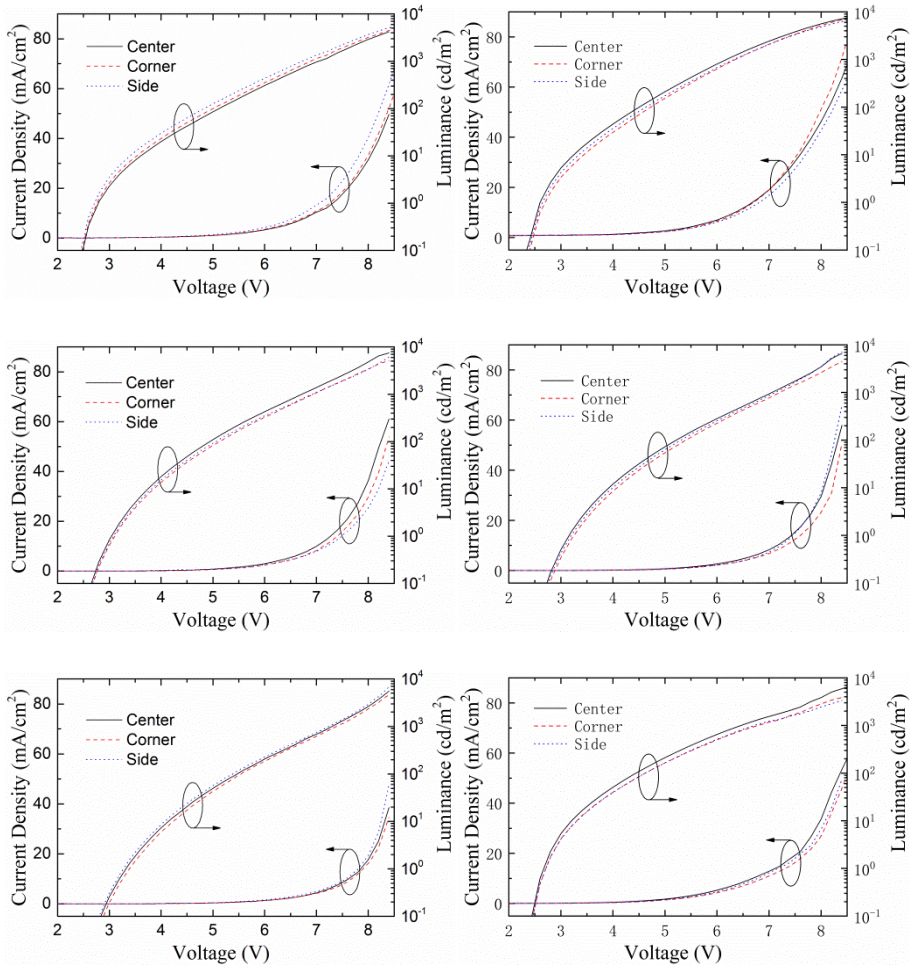


Figure S10 J-V-L curve of 18 PH1000-OLED from 6 batches.